Performance of a hard x-ray undulator at CHESS (invited)

D. H. Bilderback, B. W. Batterman, M. J. Bedzyk, K. Finkelstein, C. Henderson, A. Merlini, W. Schildkamp, Q. Shen, and J. White

CHESS, Cornell University, Ithaca, New York 14853

E. B. Blum

Laboratory of Nuclear Studies, Cornell University, Ithaca, New York 14853

P. J. Viccaro, D. M. Mills, S. Kim, and G. K. Shenoy

Advanced Photon Source, Argonne National Laboratory, Argonne, Illinois 60439

K. E. Robinson, F. E. James, and J. M. Slater

Spectra Technology, Inc., Bellevue, Washington 98004

(Presented on 30 August 1988)

A 3.3-cm period Nd-Fe-B hybrid undulator has been designed and successfully operated in the Cornell Electron Storage Ring (CESR). This 2-m-long, 123-pole insertion device is a prototype of one of the undulators planned for the Advanced Photon Source. In dedicated operation, the undulator produced the expected brightness at 5.437 GeV with the fundamental x-ray energy ranging from 4.3 to 7.9 keV corresponding to a change in gap from 1.5 to 2.8 cm.

INTRODUCTION

Undulators are periodic magnetic devices that can produce an extremely brilliant beam of x rays when operated in low-emittance storage rings. The periodic magnetic structure of an undulator produces interference effects in the emitted radiation resulting in sharp peaks in the x-ray spectral distribution. This property selectively compresses the radiation in narrowbands and enhances the fraction of the output energy spectrum that is desirable for a specific x-ray experiment. We report on the tests performed on the first undulator operating at Cornell High Energy Synchrotron Source (CHESS) using the CESR storage ring and compare our results to the calculated properties of the radiation which included the effects of nonzero emittance. This undulator is a prototype of the devices planned for the Advanced Photon Source (APS) to be constructed at the Argonne National Laboratory.

The measurements reported include an analysis of the undulator performance with regard to its energy spectra, energy tunability and polarization, source phase-space volume, and a study of the influence of the device on the operating behavior of CESR lattice. Also included are brief summaries of four scientific experiments which utilized the enhanced spectral characteristics of the undulator radiation.

I. UNDULATOR

The choice of the undulator period is intimately connected to the energy of the x rays desirable for the research activities. A period of 3.3 cm at an operational energy of the CESR storage ring between 5 and 6 GeV provides first-harmonic radiation that is tunable in the classical x-ray range from about 5 to 9 keV. This period has also been chosen for a typical undulator to be built for the APS.

The undulator is based on the Halbach hybrid design[1] using the high-field permanent magnet material, Nd-Fe-B, and high-permeability pole pieces made of vanadium permendur. The field quality in such a design depends primarily on the geometry of the pole tips. The geometrical parameters of the magnetic structure were iteratively optimized through two-dimension field computation. Three-dimensional effects were estimated in order to obtain the pole- and magnet-width required for transverse field homogeneity. The optimized undulator parameters are presented in Table I.

The 123 poles were mounted on two 2.03-m-long rigid beams ("jaws") made from aluminum. The "jaws" are mounted to the support frame through linear bearings allowing the gap to be remotely adjusted from 1.35 to 3.0 cm. The undulator frame is a modified cantilever design which allows for insertion/removal of the undulator without disturbing the vacuum beam pipe. This device, built by Spectra Technology Inc., is shown in Fig. 1. Two innovative aspects of this construction are worth noting. First, the design permitted secure mechanical clamping of all the magnets and pole pieces while allowing some degree of adjustability for tuning the field of the device. Second, the Nd-Fe-B magnets were plated with electroless nickel to avoid corrosion. Detailed

TABLE I. Optimized parameters of a Nd-Fe-B hybrid undulator.

Undulator period, λ (cm)	3.3
Magnet gap range (cm)	1.35–3.0
Maximum peak field on-axis, $B(T)$	0.53
Peak field error, $\Delta B/B$ (%)	0.3
$K = [0.934\, B(T)\, \lambda\ (\mathrm{cm})]$ range	0.4–1.6
Pole width in x direction (cm)	6.2
Pole height in y direction (cm)	3.2
Pole thickness in z direction (cm)	0.6
Magnet width in x direction (cm)	7.8
Magnetic height in y direction (cm)	3.7
Magnetic thickness in z direction (cm)	1.05
Pole-tip overhang in y direction (mm)	1.4
Overall length of undulator (m)	2.03
Number of poles	123

 0034-6748/89/071419-07$01.30

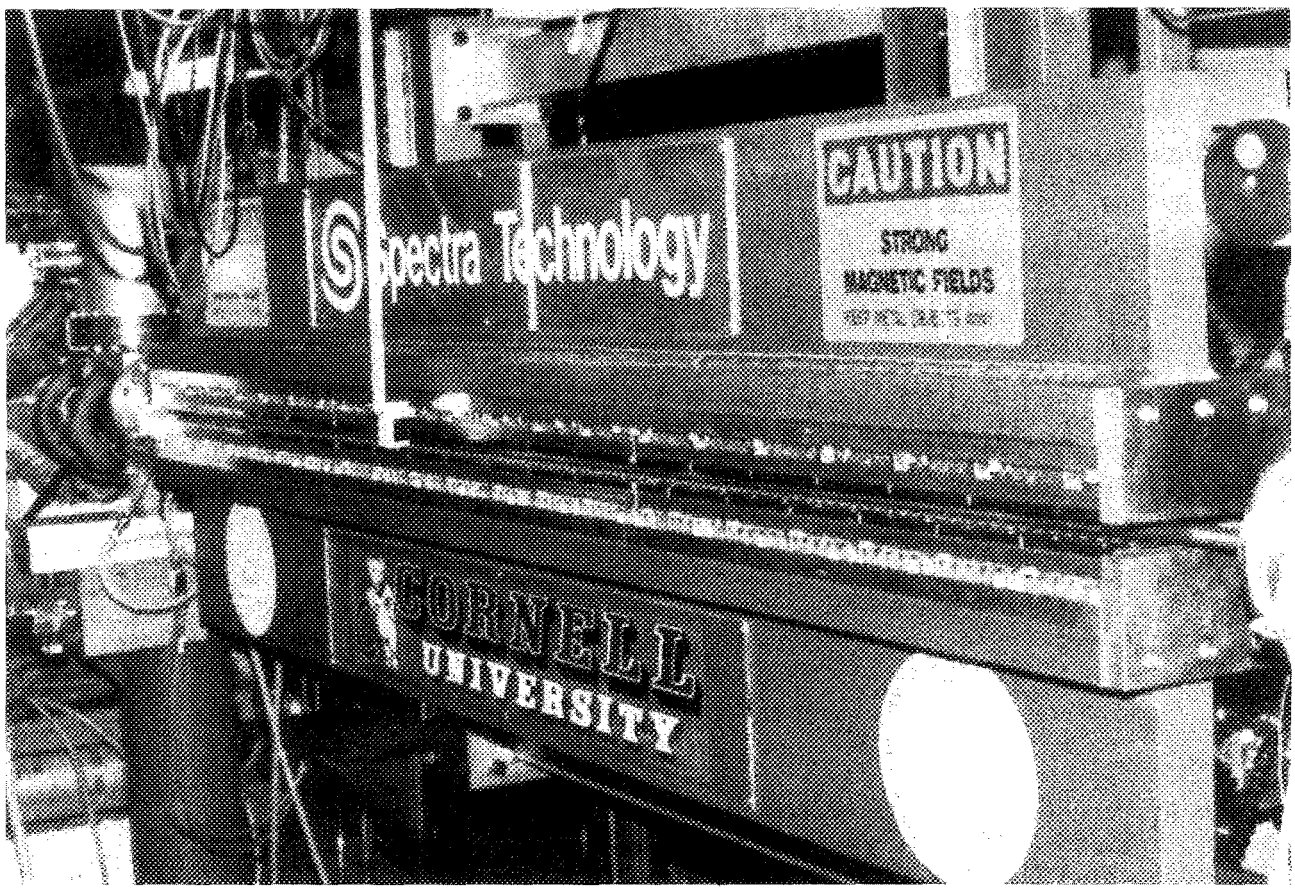

FIG. 1. The 3.3-cm-period hard-x-ray undulator with 61 periods installed in the Cornell Electron Storage Ring. The 2.03-m-long Nd-Fe-B hybrid undulator was built by Spectra Technology Inc.

magnetic measurements were performed to ensure an acceptable electron trajectory through the device. The measured on-axis field of 0.53 T at 1.35-cm gap is in agreement with the design value. The measured transverse-field roll off of less than 0.2% at $\pm$ 1.0 cm from the centerline is also consistent with the design. The integrated steering errors measured along the vertical and horizontal directions are less than 100 and 400 Gauss cm, respectively. No adjustable steering correctors were installed on the undulator. Steering correctors mounted on either ends of the straight section in CESR were never used during the undulator operation.

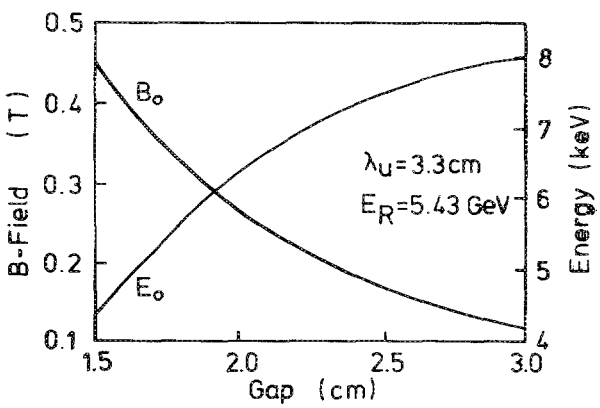

FIG. 2. On-axis peak magnetic field and fundamental x-ray energy of the undulator as a function of magnetic gap.

A stainless-steel vacuum chamber was constructed which was 2.4 m long and provided a minimum magnetic gap capability of 1.44 cm. The chamber was coupled to the storage ring with transition pieces and contained ion pumps at either end. At a gap of 1.5 cm, the peak on-axis magnetic field, B, was 0.45 T corresponding to a deflection parameter, K, of 1.4. When the ring was operated at 5.43 GeV, the first-harmonic radiation occurred at an energy of 4.3 keV. Reduction of the K value to 0.5 (by the opening of the gap to about 2.8 cm), resulted in a first-harmonic energy of 7.9 keV. The relationship between the undulator gap and the first-harmonic photon energy (and the peak on-axis field) is shown in Fig. 2.

II. OPERATION OF THE STORAGE RING CESR FOR THE UNDULATOR APPLICATION

CESR is an electron-positron storage ring operated between 4.7 and 5.5 GeV, primarily for high energy physics (HEP) research. For undulator operation, the storage ring was operated in a dedicated mode with major changes in the operational conditions. Under normal CESR colliding beam conditions, (1) the emittance used ($>$ 160 nm rad) is too large for effective undulator performance and (2) the vertical aperture of the standard vacuum chamber is too large (4.9 cm) for the undulator to function.

A new vacuum chamber was installed in the undulator straight section which restricted the inside vertical aperture

to 1.25 cm. This reduced aperture had little effect on the storage ring performance when the emittance was reduced roughly to a third of its HEP operation value. The best injection rates surpassed 10 mA/min/bunch, a value comparable to the best rates under normal HEP operation. The emittance was reduced by increasing the horizontal and vertical tunes from 9.38 to 15.42 and from 9.36 to 12.35, respectively. Tune changes were accomplished by adjusting the field strengths of the individual quadrupole magnets in the CESR lattice, all of which are under software control. Instabilities were found in the low-emittance mode if the beam was stored at 6 GeV. Such problems were less significant at 5.43-GeV operation, where injection conditions were well established and understood from previous HEP runs, and hence all measurements reported were carried out at this energy.

The design values for the horizontal and vertical electron-beam emittances were 65 and 1.0 nm rad, respectively. The emittance was routinely measured by imaging the visible light component of the synchrotron radiation from a dipole magnet onto a CCD detector (also see Sec. IV). The values of horizontal and vertical emittances previously measured [2] at 5.1-GeV operation were 50 and 1.0 nm rad. The measured values of 76 and 1.16 nm rad, respectively (at 5.437 GeV), were in reasonable agreement with the lattice design for this run. The vertical emittance was independent of the stored beam current up to 20 mA per bunch beyond which a rapid increase in the emittance was observed (Fig. 3).

The largest single-bunch current stored was 35 mA. Further injection was prevented by a beam instability which was not investigated due to limited running time.

The beam lifetime (e-folding time) at normal operating currents of 80 mA was between 200 and 300 min. Both the beam lifetime and the injection rates were found to be strongly dependent on the precise value of the vertical tune. With seven nearly equally spaced bunches (with a separation of 366 ns), the lifetime showed intermittent deterioration presumably caused by ion trapping. This was alleviated by storing only six bunches with an asymmetry provided by the position of the empty seventh bunch. The maximum stored current under these conditions was 115 mA. Operationally, 80 mA could easily be injected and stored.

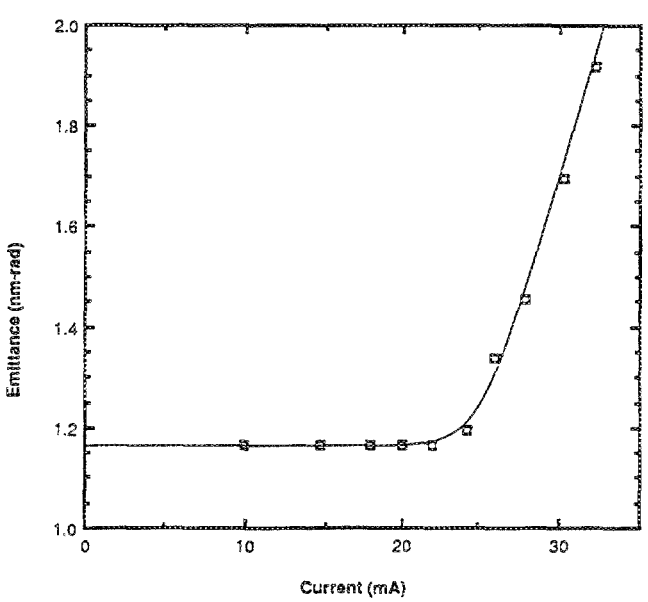

FIG. 3. Growth of vertical emittance with stored current determined from CCD detector measurements of the radiation profile. The current was stored in a single bunch.

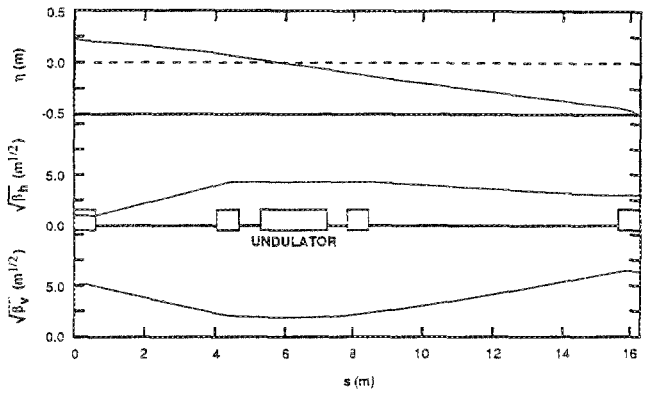

FIG. 4. Lattice functions in the undulator insertion region showing undulator and four adjacent quadrupoles. The square root of β is proportional to beam size. The horizontal dispersion function η is the displacement per unit energy error and is nearly zero in the undulator.

The lattice functions in the low-emittance mode around the undulator straight section are shown in Fig. 4. The beta function was measured around each quadrupole in the storage ring by varying its field strength and observing the effect on the tune. Quadrupole fields were then adjusted to bring the measured values of beta functions into conformance with the lattice design. The measured values of the vertical and horizontal beta functions in the straight section were 4.81 m and 20.7 m, respectively, with the change in beta with distance along the orbit being nearly zero in both directions. The lattice design values were 4.89 and 19.5 m.

There was little, if any, influence of the undulator on the storage ring operational parameters, in particular on the tune shifts. Varying the gap of the undulator magnet arrays had little effect on the stored beam.

III. SPECTRAL MEASUREMENTS

One of the most useful spectral properties of an undulator source is the spectral brilliance which is defined as the flux emitted from a unit phase-space volume of the source. In order to accurately determine experimentally the spectral brilliance, it is necessary to evaluate various contributions to the undulator source size. This subject has been discussed in detail by Brown *et al.*[3] and we will only summarize the findings in our case. The main contribution to the source size arises from the electron beam emittance and in terms of the Gaussian rms widths σ_i and σ_i' [both in the horizontal ($i=x$) and vertical ($i=y$) directions] is given by $\sqrt{\epsilon_i \beta_i}$ and $\sqrt{\epsilon_i/\beta_i}$, respectively (see Table II). Here ϵ_x and ϵ_y are electron beam emittances in the horizontal and vertical directions. Source size broadening due to dispersion effects must also be considered. In our case, the small value of the horizontal dispersion at the straight section along with a small electron energy spread adds less than $\frac{1}{2}$ % to the horizontal size of the source. The increase in the source size from

TABLE II. Measured phase-space parameters with CCD optics and with scanning slits on x-ray beam (discussed in Sec. IV).

	ϵ_x nm rad	ϵ_y nm rad	σ_x mm	σ'_x mrad	σ_y mm	σ'_y mrad
CCD optics	76	1.16	1.25	0.061	0.076	0.015
Slits	84	1.96	1.33	0.063	0.140	0.014

the radiation field describing the depth-of-field or diffraction effects[4] is estimated to be less than 1%. Hence, the electron beam size totally determines the undulator radiation source size in our case. The results of the measurements are summarized in Table II.

A. Measurement of the angle-integrated flux

The angle-integrated flux is an invariant for a prescribed operation of an undulator and can be experimentally measured. Theoretically, this quantity is obtained by multiplying the on-axis brilliance by the phase-space volume. The experimental measurement of the angle-integrated flux as a function of x-ray energy was carried out using a nondispersive double-crystal monochromator employing either silicon (111) or (311) symmetrically cut crystals. The first crystal of the monochromator was located 18.6 m from the center of the undulator source, and was cooled either by water or liquid gallium.[5] All the measurements were made with a stored beam current of less than 5 mA to make sure that the optics did not distort due to the heat load from the undulator radiation. There was a total of 2-mm beryllium and 10-cm air between the source and the detector, in addition to the helium-filled transport line. The measurements were carried out using ion chambers filled with either nitrogen or argon gas at STP. The ion-chamber currents were converted to flux assuming perfect crystal reflection properties. Software feedback ensured that data were collected at the peak of the rocking curve. These data were corrected for absorption in Be, air, and helium in the x-ray path. Figure 5 shows angle-integrated data measured with an undulator gap of 1.5 cm which corresponds to a K value of 1.4. Seven harmonics were observed in the energy spectrum. There was a large contribution to the low-energy part of this spectrum from the finite size of the source since no slits were used. The measured flux from the odd harmonics ($n = 1,3,5,7$) can be obtained from these data and is compared with the calculated angle-integrated flux in Table III.

TABLE III. Measured (Fexp) and calculated (Fcalc) angle-integrated flux (photons/s/0.1% bw/mA) at a gap of 1.5 cm ($K = 1.4$) and harmonic number $n = 1,3,5,7$.

n	E_n keV	Fexp 10^{12}	Fcalc 10^{12}	Fexp/Fcalc
1	4.25	1.1	4.6	0.24
3	12.75	1.3	1.6	0.81
5	21.25	0.4	0.5	0.80
7	29.75	0.1	—	—

In order to compare the measured angle-integrated flux at various odd harmonics with theoretical values, we have performed a numerical computation of the energy spectrum which includes the phase-space volume of the electron source. A typical brilliance spectrum for $K = 1.4$ is shown in Fig. 6. The values of angle-integrated flux at various harmonics is deduced by multiplying the theoretical values of the on-axis brilliance by the phase-space volume of the source used in these calculations. The first-harmonic radiation at 4.25 keV is severely attenuated in the path before the detector and the discrepancy reflects some of the difficulties in fully accounting for the absorption corrections. For the higher harmonics the disagreement is less than 20% and should be considered good in view of numerous experimental uncertainties.

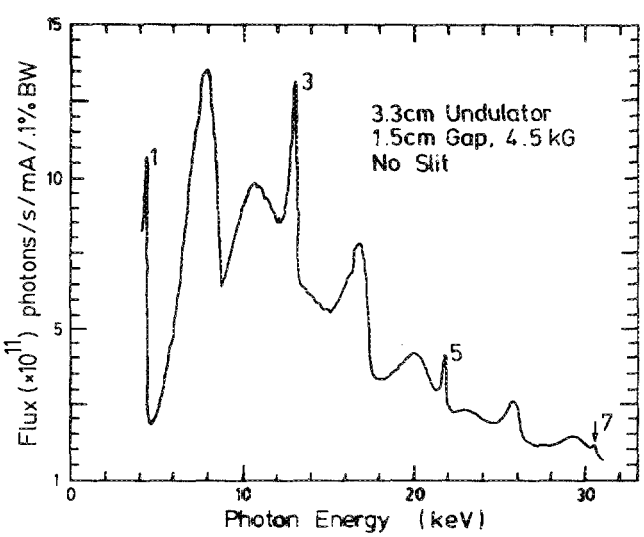

FIG. 5. On-axis angle-integrated flux observed as a function of energy with $K = 1.4$. The harmonic peaks were observed out to the seventh order.

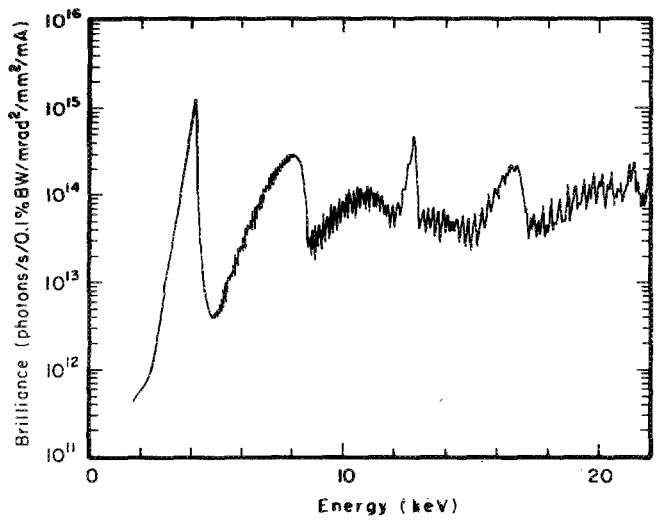

FIG. 6. Calculated on-axis brilliance as function of x-ray energy for the 3.3-cm-period undulator with 61 periods, showing various odd and even harmonics. The Monte Carlo calculations assumed $K = 1.4$ (1.5-cm gap), $E = 5.437$ GeV, $\epsilon_x = 76$ nm rad, and $\epsilon_y = 1.16$ nm rad.

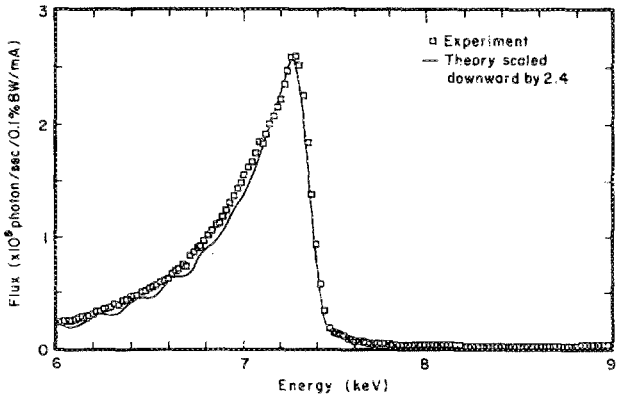

FIG. 7. Flux through 100×100 μm pinhole showing the first-harmonic energy spectrum with $K=0.54$ undulator gap. The solid curve is theory, which includes the electron phase-space dimensions, and reproduced the experiment if scaled downward by a factor of 2.4.

B. Flux measured through a pinhole

A pinhole placed along the axis of the undulator can reduce the source size seen by the detector, thus increasing the peak-to-valley ratio at each of the harmonics. Measurements were carried out by placing a square slit (100×100 μm^2) 18.5 m away from the center of the undulator. The detector was positioned another 7.5 m further downstream. The angle subtended by the pinhole was about 0.003 mrad around the undulator axis, and was smaller than the opening angle of the undulator radiation (see Table II). In these measurements, the monochromator was located immediately behind the pinhole. Figures 7 and 8 show two typical scans of the first harmonic at 7.3 keV (with $K=0.53$) and the third harmonic at 13.0 keV (with $K=1.4$). The solid curve through the data in these figures show the best fit to a theoretical calculation of the flux through the pinhole. These calculations account for the nonzero size of the source and the projection of the pinhole onto the source phase-space ellipse. In obtaining the fits, the only variable parameter used was the value of the flux at the peak of the harmonics. The fit resulted in a reduction of the theoretical value of the peak flux by a factor of 2.4. The origin of this factor is not fully understood, although vertical beam position oscillations could be the main contributor. It must be pointed out that in Fig. 7 the theoretical curve shows oscillations in the intensity due to the finite size of an undulator with a limited number of periods. These oscillations were smeared out in the data consistent with the hypothesis of electron beam motion or trajectory errors in the undulator. The full width at half intensity of the first and third harmonics shown in Figs. 7 and 8 are 400 and 200 eV. The main contribution to these widths comes from the homogeneous broadening given by $1/nN$, where N is the number of periods and n is the harmonic number. In addition, nonzero source size (σ_i and σ_i', $i=x,y$) and nonideal fields in the undulator also contributed to the observed width.

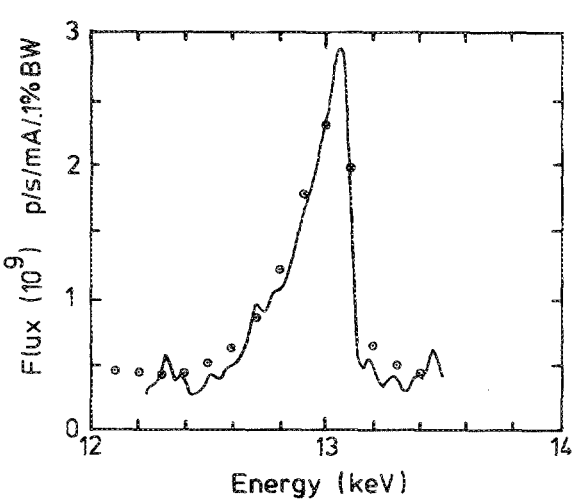

FIG. 8. Flux through 100-μm pinhole showing the third-harmonic energy spectrum with $K=1.4$ undulator gap. The solid curve is theory, which includes the electron phase-space dimensions, and reproduced the experiment if scaled downward by a factor of 2.4.

C. Polarization measurements

The angular dependencies of the polarization components of radiation from an undulator have very interesting behavior.[6] For example, while the radiation has only σ polarization in the orbital plane, the radiation above and below the plane has both σ- and π-polarization components. Measurements of polarization were carried out using an x-ray Compton scattering polarimeter similar to the design of Smend *et al.*[7] Because of the restricted time available for these measurements, the studies were limited to few data points above and below the orbital plane for the first- and second-harmonic radiation at 7.3 and 13.1 keV, respectively. The in-plane linear polarization was measured to be over 90% at both these energies. Above and below the orbital plane, the percentage of linear polarization for the second harmonic decreased monotonically with distance along the y axis, with evidence of small shoulders in the first-harmonic scans.

IV. MEASUREMENT OF ELECTRON BEAM EMITTANCE

In Sec. II, a discussion was presented regarding the contributions to the source phase space. Almost all of the contribution comes from the electron beam phase space which, in turn, is determined by the electron beam emittance. The electron beam emittance is often measured using the optical part of the synchrotron radiation emanating from the bending magnet. The result of such a measurement using the CCD optics is given in Table II.

Another way of obtaining the electron beam emittance is through the measurement of the phase-space ellipse of the hard x rays produced by the undulator. A novel method which uses scanning slits was developed for this purpose. Assuming Gaussian distributions for the positions and directions of the electrons in the beam, the source divergence and size can be described by horizontal (σ_x,$\sigma_{x'}$) and vertical (σ_y,$\sigma_{y'}$) phase-space distributions, where σ_x, σ_y and $\sigma_{x'}$, and $\sigma_{y'}$ are the spatial and angular Gaussian widths of the electrons in the beam. In phase space an x-ray constant-intensity contour is elliptical.

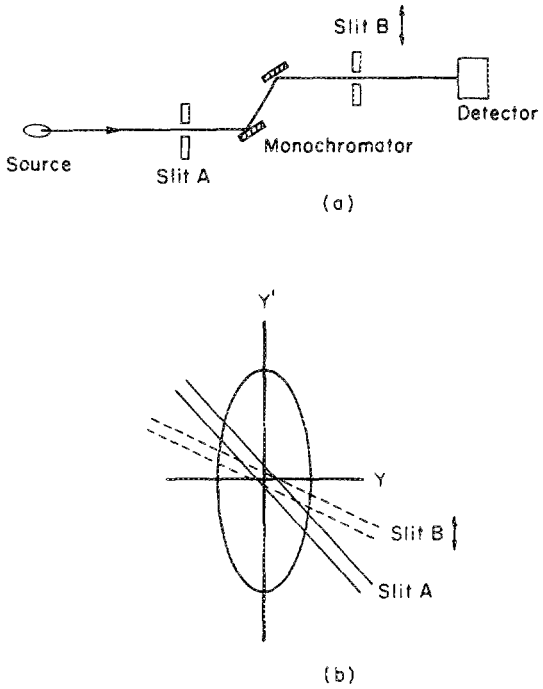

FIG. 9. (a) Schematic of vertical scanning slit apparatus. (b) Analysis proceeded by projecting the slit openings back upon the phase-space ellipse describing the source.

Two movable narrow slits were used to measure the elliptical contours [Fig. 9(a)]. In order to measure the (σ_y, $\sigma_{y'}$) contour, long horizontal slits of 25-μm opening were placed at A and B. For every position of A, a narrowband of the (σ_y, $\sigma_{y'}$) phase space is exposed as shown in Fig. 9(b). The slit B is then scanned vertically to yield the x-ray intensity distribution in band A. From the known distance of the source point to the slits, the intensity information can be converted to obtain the intensity distribution at the source. The entire vertical phase-space ellipse is mapped by repeating the procedure at various positions of slit A. The entire procedure is then repeated with 100-μm-wide vertical slits located at A and B to trace the horizontal phase-space ellipse. The horizontal and vertical phase-space ellipses obtained in this way are shown in Fig. 10. The phase-space parameters are given in Table II. From these values the emittance of the storage ring can be determined as discussed in Sec. II.

It is interesting to compare the agreement between the values of the phase-space sizes obtained from the CCD optics and scanning slit measurements. The only major discrepancy is in the vertical source size. The increase in the vertical beam size for the slit data may be due to beam motion or instabilities over the 2- to 3-min-long periods needed to perform the x-ray scanning slit measurements. The CCD measurement, on the other hand, took only 1 ms of time. The factor of 2 larger effective vertical source size in the undulator region obtained from the scanning slit measurements could also account for the reduction in the brilliance discussed in Sec. III B.

V. UNDULATOR POWER AND POWER HANDLING

The total power (in watts) radiated from an undulator of length L (in m) is given by

$$P = 0.633\, E^2 B^2 I L,$$

where E is the energy of the stored electrons in GeV, B is the peak on-axis magnetic field in the undulator in Tesla, and I is the stored current in mA. With the gap of the undulator set at 1.55 cm ($B = 0.42$ T), the device produced 6.7 W/mA.

The power delivered by the undulator with a stored current of 68 mA was 456 W. Of this, only 66% or 301 W of power can reach the first optics due to absorption in the prefilters and Be windows. The measurement of the power reaching the optics was carried out by using calorimetric methods in which the radiation from the device was fully collected in a reentrant cup-shaped copper block. The increase in the temperature of this suspended block over a fixed exposure time to the radiation was used to obtain the incident power. The temperature of the copper block increased by 23.6 °C in 10 s. The calorimeter detected a total of 260 W which was 86% of the expected value.

Our ability to handle this power on the first optical component was vital to the success of planned scientific research. Hence, one of the foremost efforts was to develop well-cooled optics. Although the total power is modest, the power density is very high due to the small size of the undulator

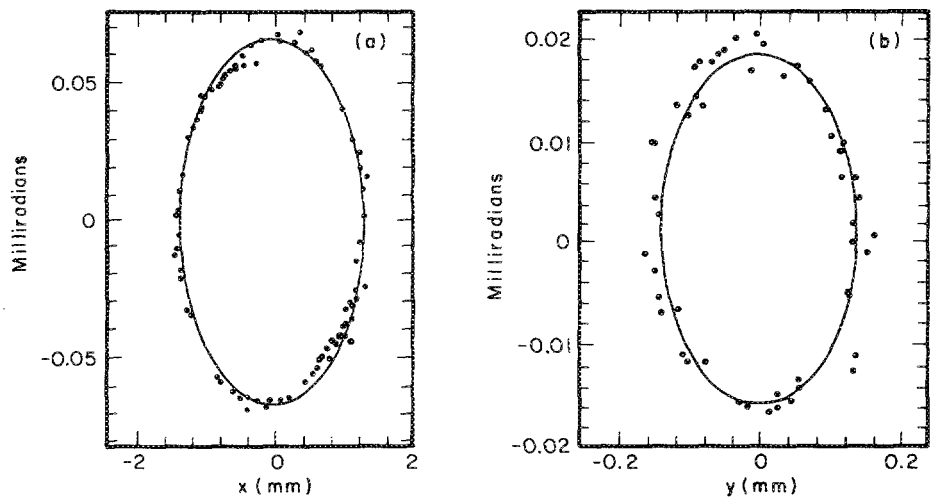

FIG. 10. (a) Horizontal and (b) vertical-phase-space ellipses determined by scanning slit measurements.

beam. It was found that the radiation heat load from the undulator distorted the large water-cooled silicon optics for beam currents above 5 mA (22 W absorbed power). On the other hand, cooling the silicon optics with liquid gallium made it possible to utilize the full power of the undulator beam with as much as 80 mA of current stored in the ring.[5]

VI. USE OF UNDULATOR RADIATION IN SCIENTIFIC STUDIES

Several experiments were performed using the undulator radiation. These experiments provided a benchmark for performance comparisons between undulator beams and more conventional sources. One of the experimental studies undertaken was a fluorescence microprobe analysis of meteorite and other mineral samples.[8] Undulator radiation lends itself naturally to microprobe studies due to the high brilliance of the emitted beam. The unmonochromatized beam was collimated through a $10\times 10\ \mu m^2$ square aperture and allowed to impinge on the sample. By rastering the sample and measuring the fluorescence with an energy resolving detector, element-specific spatially resolved maps of the sample were produced. One significant finding was that the minimum detectable level (MDL) when using an undulator beam was found in some cases to be about a factor of 10 less than the MDL using a bend magnet source.

A second group of experiments involved x-ray standing waves. The two experiments performed each employed nonstandard variations of the normal standing wave technique. In one case,[9] Bragg diffraction from a nonperfect high T_c superconducting crystal was used to produce the standing wave field and in the other,[10] the standing wave field was produced at a charged liquid/solid interface by using total external reflection. In order to generate a sufficiently strong standing wave pattern, both experiments required a small beam cross section of $\sim 0.01\ mm^2$. For this cross-sectional area, in the 8–12 keV region, the undulator radiation generated two orders of magnitude increase in the detected fluorescence signal over a comparable setup on a bend magnet source.

The final experiment provided perhaps the most dramatic display of the advances that can be made using undulator radiation. Unmonochromatized undulator radiation was allowed to strike a protein crystal after passing through a 300-μm-diam collimator[11] and a fast shutter.[12] With 35 mA of electrons stored in a single bunch, a transmission Laue diffraction pattern of lysozyme was obtained with the x rays from the single bunch of electrons. The diffraction pattern was recorded on storage phosphors (image plates) rather than standard x-ray film, in an exposure time corresponding to the bunch duration of 120 ps. Previous attempts at producing short exposure Laue diffraction patterns have been limited to the hundreds of microseconds regime. The undulator radiation has provided a quantum leap in the decrease in exposure time required to produce a diffraction pattern. This feasibility demonstration opens up many new possibilities to investigate dynamic processes in material and biological sciences in the future.

ACKNOWLEDGMENTS

One of the authors (DMM) gratefully acknowledges support from the Guggenheim Foundation for this work. The authors (PJV, DMM, and GKS) would also like to thank George Brown and Stanford Synchrotron Radiation Laboratory for many useful suggestions regarding the beam emittance measurements.

This work supported by the U. S. Department of Energy, BES-Materials Sciences, under contract no. W-31-109-ENG-38 and National Science Foundation, under contract no. DMR-87-19764.

[1] K. Halbach, J. Phys. (Paris) **C1-44**, 211 (1983).
[2] E. Blum, Cornell Laboratory for Nuclear Studies, Internal Report CON 86-4 (16 April 1986).
[3] Brown *et al.*, in *Proceedings of the 1987 IEEE Particle Accelerator Conference*, edited by E. R. Lindstrom and L. S. Taylor (IEEE, Pittsburgh, PA, 1987), p. 461.
[4] K-. J. Kim, Nucl. Instrum. Methods A **246**, 71 (1986).
[5] D. Bilderback, C. Henderson, J. White, R. K. Smither, and G. A. Forster, these proceedings; R. K. Smither, G. A. Forster, D. H. Bilderback, M. Bedzyk, K. Finkelstein, C. Henderson, J. White, L. E. Berman, P. Stefan, and T. Oversluizen, these proceedings.
[6] G. K. Shenoy, P. J. Viccaro, and D. M. Mills, Argonne National Laboratory Report, ANL-88-9 (February 1988).
[7] F. Smend, D. Schaupp, H. Czerwinski, A. H. Millhouse, and H. Schenk-Strauss, Nucl. Instrum. Methods A **241**, 290 (1985).
[8] M. Rivers, S. R. Sutton, and B. M. Gordon (to be published).
[9] S. M. Durbin and M. J. Bedzyk (to be published).
[10] M. J. Bedzyk, G. M. Bommarito, M. Caffrey, and T. Penner (to be published).
[11] D. M. E. Szebenyi, D. Bilderback, A. LeGrand, K. Moffat, W. Schildkamp, and T.-Y. Teng, Trans. the Am. Crystallogr. Assoc. **24** (in press).
[12] A. D. LeGrand, W. Schildkamp, and B. Blank, Nucl. Instrum. Methods A **275**, 442 (1989).